Behaviour of a loose silty sand under static and cyclic loading conditions

Denis LeBoeuf[1,*]

[1]Department of Civil and Water Engineering, Université Laval, Québec, Qc, Canada

Abstract. In recent years, considerable progress have been made in the study of liquefaction and flow failures with the introduction of the notion of steady-state of deformation and "collapse" envelope. These concepts are increasingly used in seismic stability analysis of slopes or embankments. However, as most of these studies were carried out on clean sands in the triaxial apparatus, one may question the general applicability of these results to practical conditions as several factors such as anisotropy, fines content, undrained strength anisotropy, boundary deformation conditions, stress history, etc. may play an important role. In this paper, the behaviour of the same soil, a loose silty sand, is compared for different loading and testing conditions: drained and undrained triaxial compression tests, drained and constant volume monotonic and cyclic direct simple shear (DSS) tests. Results allow to identify similarities and differences, in terms of undrained initial and steady-state shear strength and modes of undrained failure between triaxial and DSS test conditions and show that liquefaction in DSS cyclic tests is an instability triggered by shear failure developing once the friction corresponding to the characteristic envelope, as identified in the monotonic test, has been mobilized.

1 Introduction

In recent years, considerable progress have been made in the study of liquefaction and flow failures with the introduction of the notion of steady-state of deformation and "collapse" envelope [1-4]. Practical procedures for using steady-state strength concepts in stability analysis of slopes or embankments are now available to the design engineer [5]. These studies have notably shown that the effective stress conditions during the steady-state of deformation define a unique strength envelope valid for both static and cyclic loading conditions. However, as most of these studies were carried out on clean sands in the triaxial apparatus, one may question the general applicability of these results to practical conditions where several factors such as fines content, undrained strength anisotropy, boundary deformation conditions, stress history, etc. may play an important role. At a more fundamental level, failure and liquefaction in sands under dynamic loading are complex nonlinear phenomena for which several aspects remain to be clarified [6-8].

In this paper, the behaviour of a loose silty sand, is compared for different loading and testing conditions: drained and undrained triaxial compression tests, drained and constant volume monotonic and cyclic direct simple shear (DSS) tests. A first objective is to identify similarities and differences, in terms of undrained-initial and steady-state shear strength and modes of undrained failure. A second objective is to use triaxial and DSS tests results to study and characterize yielding, failure and cyclic mobility (or initial liquefaction) as an undrained instability mechanism and to relate the observed behaviour with the static effective strength parameters.

2 Soil description and testing program

The soil used in this study is a natural silty sand, similar to most core material of earth dams in Quebec. Grain size distribution curve is shown in Figure 1 and index properties are listed in Table 1. Three series of tests were carried out. The first series of tests was conducted to study the behaviour of the silty sand under isotropically-consolidated drained (CIDc) and isotropically and anisotropically-consolidated undrained triaxial compression (CIUC/CAUC tests) with strain-controlled loading. The second series included drained and constant volume (equivalently undrained) direct simple shear tests. Finally, a third series of tests were conducted to study the cyclic behaviour of this soil under constant volume cyclic simple shear conditions. The NGI apparatus [9] was used in all tests.

Since undrained soil behaviour is controlled not only by the density but also by the effective stresses, which will determine the contractant or dilatant behaviours for a given density, the approach has been to prepare all the specimens by the same technique, light tamping in order to simulate embankment fill, at the same initial low density and let the density adjust under the consolidation, thus creating essentially a normally consolidated (N.C.) condition for the silty sand, so no tests has exactly similar void ratio (or D_r) values at start of the shear phase.

Triaxial tests specimens were prepared in a cylindrical mold by light tamping of soil specimens at field moisture content (10% - 11%). For all triaxial or DSS specimens, an initial dry density of 1.60 g/cc was targeted before consolidation (D_r = 39%). All technical details on

* Corresponding author: denis.leboeuf@gci.ulaval.ca

specimen saturation, consolidation, etc can be found in [10].

Table 1. Summary of index properties.

Property	Value
Unified Classification	SM
D_{50}	0.16 mm
c_u	17
% clay-silt	24.6
e_{max}	0.942
e_{min}	0.28
$\rho_{d\text{-}maximum}$	2.10 g/cm^3
G_s	2.70

Cyclic simple shear tests were carried out on a modified version of the NGI device. The sinusoidal horizontal cyclic shear force is applied by a double entry pneumatic piston at a frequency of 0.1 Hz.

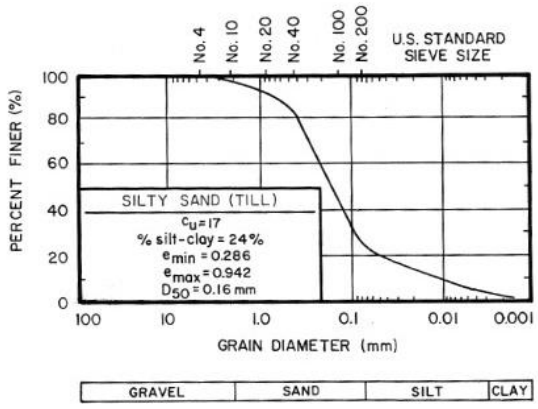

Fig. 1. Grain size curve for the silty sand

3 Test results

3.1 Monotonic triaxial tests

Stress-strain-pore pressure curves, for undrained triaxial tests, and stress-strain volumetric deformation curves for drained tests, are presented in Figures 2 and 3, respectively. Effective stress paths are plotted in Figure 4.

Note that the results of four undrained triaxial tests are presented on Figure 2. It is only the three tests on isotropically consolidated specimens (dashed lines on Figure 2) which are examined for the moment.

The drained (CIDC) triaxial tests (Figure 3) show a typical contractant behaviour and the maximum deviatoric stress had not yet been mobilized at the end of the tests at around 8% of axial deformation. The friction angle mobilized at the end of the tests was around 30° and still increasing.

Undrained, strain-controlled, triaxial compression shear has produced an initial peak resistance at a very low axial strain of about 0.6% followed by rapid strength loss (Figure 2). The strength and pore pressure tend to stabilize at large strain. This could be identified as the steady-state of deformation. The initial peak strengths defines a linear envelope at a mobilized friction angle of 20°. At large strains, the stress paths (see Figure 4) stabilized on an envelope defined by a friction angle of about 36°. Results from anisotropically-consolidated Test CAUC-01 also clearly illustrate however that a loose soil specimen submitted to an initial shear stress still has a high strength reserve in drained shear but will withstand only a very small undrained loading for failure (Figure 4). Similar results have been presented by others [12, 13].

The undrained shear strength ratio, S_u/σ'_{vc}, is, on the average, equal to 0.24. For the same testing conditions, one would expect such a ratio, for a normally consolidated clay, to be around 0.30 - 0.35 [11].

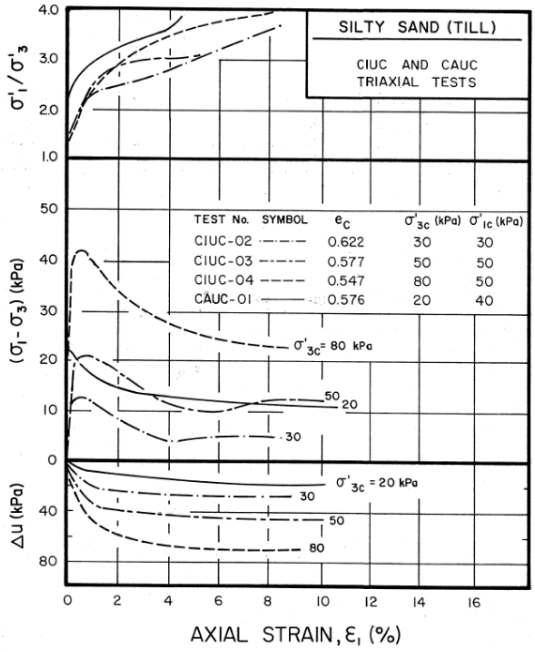

Fig. 2. Stress-strain, pore pressure-strain and σ'_1/σ'_3 strain curves from undrained triaxial tests on loose silty sand.

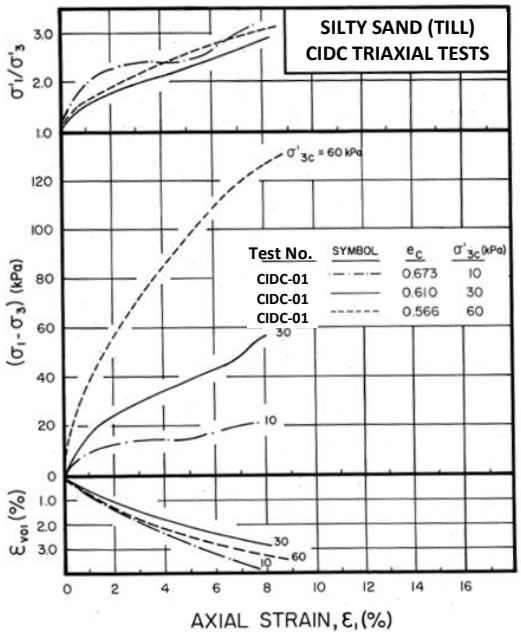

Fig. 3. Stress-strain, pore pressure-strain and σ'_1/σ'_3 strain curves from drained triaxial tests on loose silty sand.

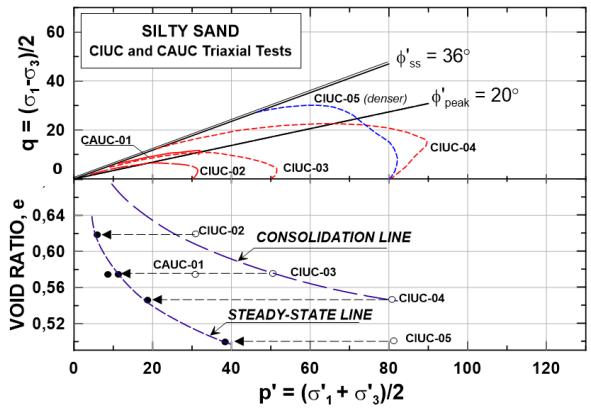

Fig. 4. Effective stress paths from CIUC and CAUC triaxial tests on loose silty sand.

3.2 Monotonic direct simple shear tests (DSS)

Figure 5 plots the horizontal shear stress (τ_h), the mobilized friction on the horizontal plane and the effective vertical stress change as function of the horizontal shear strain for the constant volume simple shear tests carried on normally consolidated specimens prepared, before consolidation, at ρ_{do} = 1.60 g/cc (or D_r ≈39%). A second series of tests was carried out on denser specimens of the same silty sand but not in a normally consolidated state (see Figure 6).

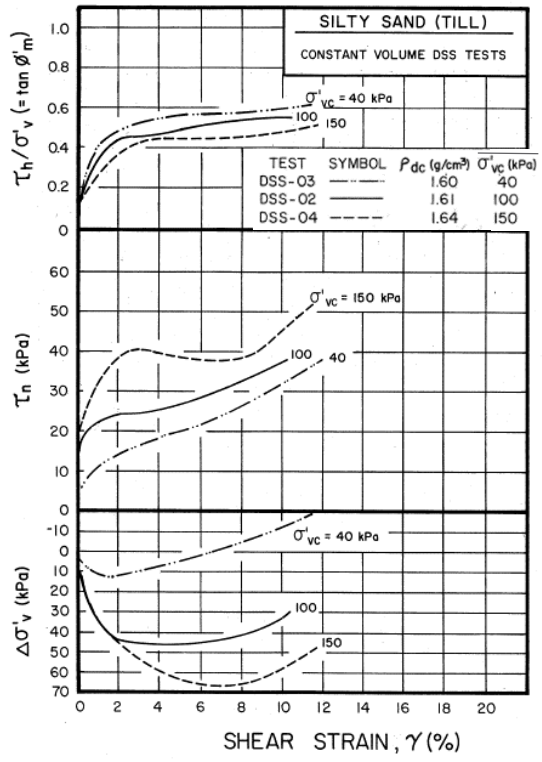

Fig. 5. Mobilized friction on the horizontal plane (tan ϕ'_m = τ_h/σ'_v), horizontal shear stress (τ_h), and effective vertical stress change ($\Delta\sigma'_v$) versus shear strain (γ) from constant volume direct simple shear (DSS) tests

The normally consolidated specimen at 100 kPa (see Figure 5) does not really show a well-defined peak but only a limited plateau in the stress-strain curve after which dilatancy and strain-hardening are observed. The mobilized friction when reaching the plateau is equal to 20°-22° and to 24° at the onset of dilatancy. This latter friction angle (24°) will also be called the « *characteristic friction angle* », as introduced by [14].

The specimen consolidated at 40 kPa does not show a plateau in the stress-strain but only a slight bend when the volumetric behaviour changes from contractant to dilatant. For all tests, this change is clearly seen on the stress vector plots (Figure 6). The characteristic friction angle coincides with the line joining the turning points in the effective stress vector plots. However, it is only when the shearing is started far enough of the turning point line that a well-defined plateau in the stress-strain curve is observed. The phase of dilatancy, initiated in the DSS at a mobilized friction of 24° was not however observed in the triaxial tests reflecting the influence of different boundary conditions on soil behaviour.

The denser specimens (Figure 6) were initially contractant but showed a strong dilatancy at fairly low shear strains. The contractant phase was not sufficient to develop limited liquefaction nor a plateau in the stress-strain curve. The initiation of dilatancy occur at a mobilized friction angle lower than in the loose specimens.

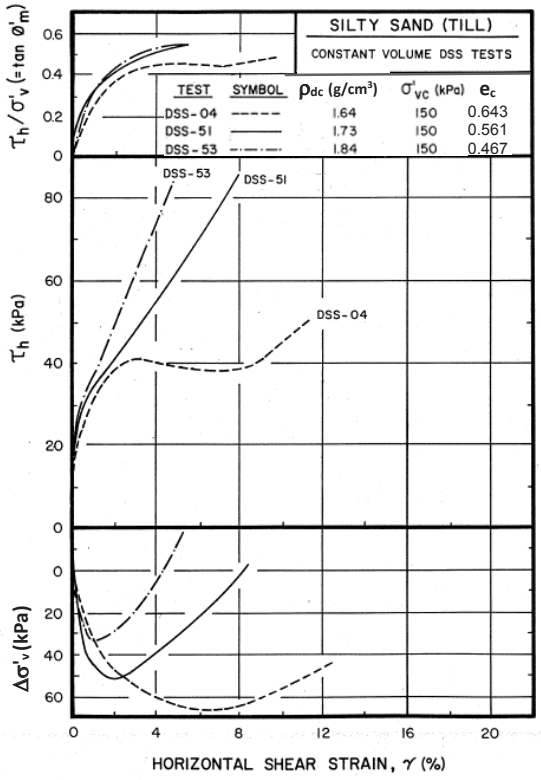

Fig. 6. Mobilized friction on the horizontal plane (tan ϕ'_m), horizontal shear stress (τ_h) and effective vertical stress change ($\Delta\sigma'_v$) versus shear strain (γ) from constant volume direct simple shear (DSS) tests on dense specimens of silty sand.

In the DSS, which has boundary conditions closer the plane strain, a plateau in the shear stress-shear strain curve develops only if the shearing starts far enough on the loose side of the turning point line (initiation of dilatancy). In other words, the soil needs to be loose enough to develop sufficient contractancy to show a limited liquefaction failure mode.

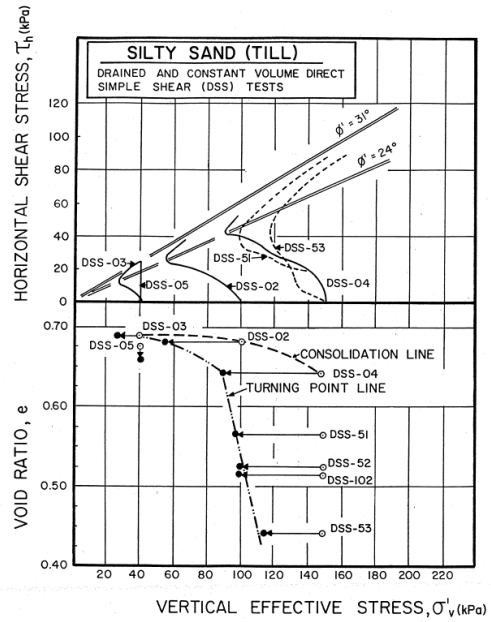

Fig. 7. Effective stress vector plots from constant volume DSS tests on loose (normally consolidated) and denser silty sand.

3.3 Cyclic direct simple shear (DSS) tests

3.3.1 Cyclic strength curves (S-N curves)

Two series of cyclic tests were carried out on the loose N.C. silty sand, under vertical consolidation pressures of 40 and 150 kPa respectively. The results are presented in Fig. 8 in the form of the classical S-N curve. The cyclic strength was defined using the initial liquefaction criteria (r_u = = $\Delta u/\sigma'_{vc}$ =100%) or the 5% (*peak-to-peak*) cyclic strain criteria.

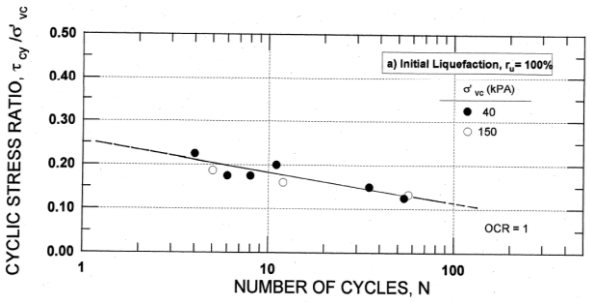

Fig. 8. Cyclic shear strength of a loose silty sand at vertical consolidation pressures σ'_{vc} of 40 and 150 kPa.

Both criteria yield around the same number of cycles, illustrating that in loose sand or silty sand, large strain develop rapidly at failure. It is of interest to note that linearly extrapolating the S-N curve to the first cycle yields a normalized strength ratio approximately equal to the ratio determined in monotonic tests. Strain and pore pressure build-up for the 3 tests consolidated at 150 kPa are shown in Figure 9. As can be seen in the effective stress vector plot of cyclic DSS test CyDSS-22 (Figure 10), the pore pressure build-up continuously reduces the effective stresses and brings the specimen closer to the static failure envelope. For the test CyDSS-23, cyclic shear strains remain very low, up to cycle 52. It is only when the pore pressure starts to accelerate again that large cyclic shear strains starts to develop. As will be seen below, this remarkable behaviour is typical of all cyclic tests on loose silty sand and can be explained by considering the effective strength parameters. Basically, the failure mode in cyclic DSS tests is closer to cyclic mobility with, however, no apparent limits in shear strain amplitude.

3.3.2 Yielding, failure and instability

As discussed above, the pore pressure and strain development in cyclic DSS tests on loose sand is characterized by a threshold behaviour: once a critical number of loading cycles is reached, both pore pressure and shear strain start to increase at an accelerating rate.

In this section, we investigate if this threshold behaviour could be explained in terms of effective strength parameters. The question to be answered is whether or not the acceleration in strain or pore pressure observed in all cyclic tests on loose silty sand is related to the mobilization of a critical level of friction in the soil. The approach used in this section is to relate the development of horizontal cyclic shear strain (γ_{cy}) to the mobilization of friction in the horizontal plane (tan ϕ'_m). Resulting γ_{cy}-tanϕ'_m curves for all cyclic DSS tests carried out in Figures 11 and 12.

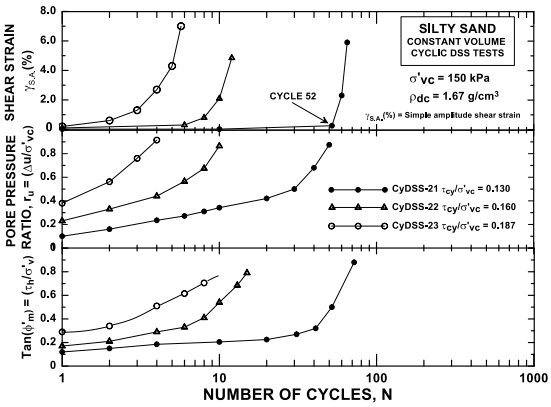

Fig. 9. Development of excess pore pressure and shear strain with number of cycles for 3 cyclic DSS tests on loose silty sand

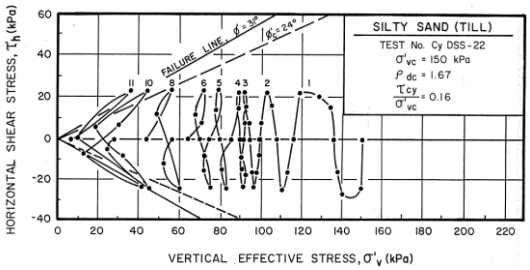

Fig. 10. Effective stress vector plot - Test CyDSS -22.

A remarkable acceleration in the development of shear strains (static or cyclic) as a function of tanϕ'_m can be observed once this critical threshold of mobilized friction (tanϕ'_{mc}) is exceeded (in Figsures 11 and 12).

Basically, in cyclic tests, the control is « *lost* » and the soil becomes unstable. This condition is considered to be failure. It is identified for each test in Figures 11 and 12

by the letter « F ». Moreover, on these figures, it may also be possible to define a second level of mobilized friction, prior to failure, below which there is, practically, no deformation at all. This first break or flexion in the γ_{cy} - $\tan\phi'_m$ curve reflects the « yielding » or initiation of the failure process in the soil specimen and is identified by letter « Y » in Figures 11 and 12.

The yield and failure points (« Y » and « F » points) are unambiguously defined for each test. The only exception is the cyclic test CyDSS-03 (Figure 12), in which the very high cyclic stress ratio used in the test brought the specimen to failure in the first cycle so that the yield point cannot clearly appear. In all tests, yielding first occurs at an equivalent angle of friction of about 10° - 12°.

Failure associated with the critical threshold of mobilized friction, occurs at a friction angle of 24° ($\tan\phi'_{mc} \approx 0.44$ - 0.45). This critical friction angle in cyclic tests (24°) is equal to the characteristic friction angle observed in monotonic tests. One should note, also, that the acceleration in pore pressure build-up of the r_u-N curve (see Figure 9) also coincides with the mobilization of the critical level of friction (24°).

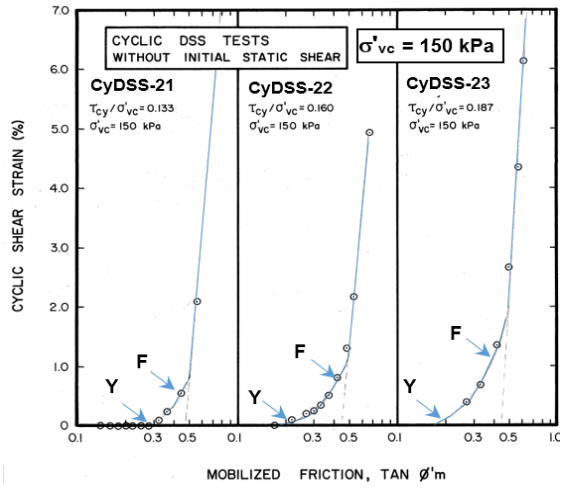

Fig. 11. Cyclic shear strain versus mobilized friction in the horizontal plane for cyclic DSS at σ'_{vc} = 150 kPa.

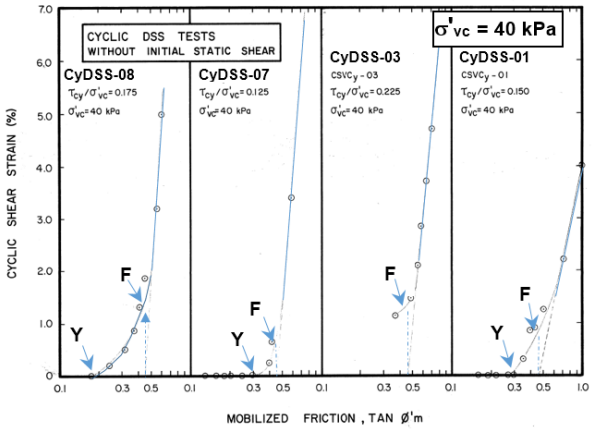

Fig. 12. Cyclic shear strain versus mobilized friction in the horizontal plane for cyclic DSS at σ'_{vc} = 40 kPa.

3.3.3 The question of anisotropy

The fundamental aspects of undrained shear strength and liquefaction for granular material have generally been examined with the triaxial test [15]. It is known however that the undrained shear strength of material is strongly stress-path dependent and varies significantly with the direction and orientation of the applied shear stress (stress-system anisotropy). It is then important for engineering applications that undrained behaviour be observed in tests which simulate as closely as possible the field conditions. The cyclic DSS test is generally considered to better simulate field conditions and, for cyclic mobility failures, its results are generally applied without any correction. This discussion first examines the similarities or differences in the soil behaviour during the undrained triaxial and DSS tests presented in this paper.

In monotonic undrained shear on the normally consolidated specimens, an initial yield and failure have been observed both in the triaxial and in the DSS. In both tests, the plateau in the stress-strain curves appears as a transition towards a higher mobilized friction and the initial undrained shear strength characterizes the maximum shear stress level during that transition. The stress level during that transition (peak strength) or the friction mobilized at peak strength varies with the specimen density and is strongly stress path dependent as evidenced by the comparison of the undrained strength ratios, (S_u/σ'_{vc}), between the triaxial tests (0.23) and in the DSS (0.275).

In the triaxial, for both the isotropically- and anisotropically-consolidated specimens, the failure, followed by strain-softening brings ultimately the soil to its steady-state condition. The friction angle at steady-state is 36° for the silty sand. In the DSS, the monotonic stress vectors show, after an initial yield at a friction angle of 10°-12°, a sharp turning point marking a change from a contractant to a dilatant phase. This turning point defines the characteristic friction angle. This well-defined turning point in the DSS effective stress vector plots of loose specimens appears as a striking difference when compared to the triaxial stress path which ends at the steady-state condition. This difference appears to be related to the different boundary conditions in the two tests, especially in terms of deformation allowed during shear.

In all DSS cyclic shear tests, a loss of stability is observed when the effective stress vector touched the 24° dilatancy envelope. Failure is characterized by a rather abrupt acceleration of the shear strain and pore pressure and by the appearance of dilatancy loops in the stress vector plots. Thus, when cyclic shearing is started far enough of the dilatancy line, failure in monotonic or cyclic tests is governed by the same 24° dilatancy friction envelope which appears constant for a giving soil. Once the characteristic angle is mobilized, the soil is in very unstable condition and the turning point in the effective stress vectors coincide with an acceleration in the shear strain.

The failure in the cyclic tests at the characteristic angle reduce the shear modulus as evidenced by the shear strain acceleration. Initial liquefaction and cyclic mobility are

not causing the failure, but are triggered by an undrained failure which can develop, depending of the initial stress level, for a fairly low pore pressure increase. While only monotonic triaxial tests were carried out, they do indicate that, at least, static liquefaction can be triggered for a very small pore pressure increase if the initial static shear stress is high enough.

4 Conclusion

The general objective of this paper was to study liquefaction and undrained failure mechanisms for the same loose (normally consolidated) silty sand subjected to a variety of loading and testing conditions. Static triaxial and direct simple shear (DSS) tests and cyclic DSS tests were conducted on this loose silty sand. Basically, the testing program was designed to answer the following two questions: a) are there any effects due to anisotropy or deformation boundary conditions? b) Using triaxial and DSS tests results, is it possible to study and characterize yielding, failure and cyclic mobility (or initial liquefaction) as an undrained instability mechanism and to relate the observed behaviour with the static effective strength parameters? In other words, is it possible to better define the effective stress conditions leading to the initiation of liquefaction or cyclic mobility? With respect to the first question, static and cyclic DSS and triaxial testing, on a loose normally consolidated silty sand, has shown that the behaviour and the modes of undrained failure are strongly influenced by the test type, anisotropy and displacement boundary conditions. For engineering applications, these factors should be taken into account as undrained behaviour should be only observed in tests which simulates as closely as possible the field conditions. More specifically, it was found that undrained shear strength ratios (0.275 (DSS) vs 0.24 (triaxial), effective strength parameters (specifically the dilatancy friction angle $\phi_c' = 24°$ (DSS) vs 36° (triaxial) and stress-strain relationships for the same soil (under similar pressure and stress history conditions) are strongly dependant of the test type and boundary conditions (strain-hardening for DSS tests and strain-softening for triaxial tests).

With respect to the second question, it was found that under simple shear strain conditions, static or cyclic initiation of liquefaction is a loss of stability or undrained failure in the specimen and is controlled by an effective strength envelope, the characteristic friction angle, simply described by Mohr-Coulomb parameters. A key characteristic of the undrained and drained simple shear behaviour is the acceleration in strain and pore pressure once a critical level of mobilized friction ($\tan \phi'_{mc}$), on the horizontal plane, is mobilized within the specimen. The value of $\tan \phi'_{mc}$ for the soil used in this study is 0.44-0.45 and corresponds to the characteristic friction angle [14] of 24°, defined in monotonic tests by the change from a contractant behaviour to a dilatant behaviour.

Interpretation of our test results suggest that the two-phase « (1) collapse (2) steady-state flow » picture proposed by some authors [4] mainly from triaxial tests results do not correctly reproduce the essential characteristics of the liquefaction process. It rather appears that complete liquefaction or cyclic mobility failures may be divided in three distinct phases: the initial or elastic phase, with elastic pore pressure response, followed by a transitional non-linear yielding phase, which really marks the beginning of the structural collapse of the soil skeleton, and finally the loss of stability, characterized by an important increase in strain and pore pressure development. This is failure in the engineering sense. In DSS tests, the loss of stability invariably occur at mobilized friction angle of 24°, independent of σ'_{vc}, the mode of loading (cyclic versus monotonic) and the equivalent drainage conditions.

We thank G. Lefebvre (Université de Sherbrooke), J. Chahde (Hydro-Quebec) and the late J.-P. Lebihan for very helpful discussions.

References

1. G. Castro, S.J. Poulos, J.W. France, J.L. Enos, Geotechnical Engineers Inc., 326 (1982)
2. S.J. Poulos, J. Geot. Eng., ASCE, **107**, 553-556 (1981)
3. S.J. Poulos, G. Castro, J.W. France, ASCE, J. Geot. Eng., **111**, 553-562 (1985)
4. J.A. Sladen, R.D. D'Hollander, J. Krahn, Can. Geotech. J., **22**, 4, 579-588 (1985)
5. W.F. Marcuson, M.E. A.G. Hynes, Franklin, Earthquake Spectra, **6**, 3, 529-572 (1990)
6. J.E. Andrade, A.M. Ramos, A. Lizcano, Acta Geotechnica, **8** 5, 525-535 (2013)
7. K. Been, M. G. Jefferies, Can. Geotech. J. **41**, 972–989 (2004)
8. D. LeBoeuf, "Instability and Liquefaction in a Loose Glacial Till Under Isotropic and Anisotropic Stress States", 16th Eur. Conf. Earth. Eng., Thessaloniki, Greece (2018)
9. L. Bjerrum, A. Landva, Geotechnique, **16**, 1, 1-20. (1966)
10. D. Leboeuf, "Soil liquefaction as undrained instability", in preparation (2018)
11. M. Jamiolkovsky, C.C. Ladd, J.T. Germaine, R. Lancellota, Proc.*11th Int. Conf. Soil Mechanics & Foundation Engineering*, San Francisco, **1**, 57-153, (1985)
12. V.N. Georgiannou, J.B. Burland, D.W. Hight, Geotechnique, **40**, 3, 431-449, (1990)
13. S.L. Kramer, H.B. Seed, J. Geot. Eng., ASCE, **114**, 4, 412-430 (1988)
14. P. Habib, M.P. Luong, "Sols pulvérulents sous chargements cycliques", Séminaire Matériaux & Structures sous Chargement Cyclique, École Polytechnique, Palaiseau, (1978)
15. R. Mohamad, R. Dobry, J. Geot. Eng., ASCE, **112**, 2, 941-958 (1986)